

Proceedings of the 16th Czech and Slovak Conference on Magnetism, Košice, Slovakia, June 13–17, 2016

X-Ray Diffraction Study of $\text{CeT}_2\text{Al}_{10}$ ($T = \text{Ru, Os}$) at Low Temperatures and under Pressures

Y. KAWAMURA^{a,*}, J. HAYASHI^a, K. TAKEDA^a, C. SEKINE^a, H. TANIDA^b, M. SERA^b,
S. NAKANO^c, T. TOMITA^d, H. TAKAHASHI^e AND T. NISHIOKA^f

^aMuroran Institute of Technology, Muroran, Hokkaido 050-8585, Japan

^bHiroshima University, Higashi-Hiroshima, Hiroshima 739-8530, Japan

^cNational Institute for Materials Science, Tsukuba, Ibaraki 305-0044, Japan

^dISSP, University of Tokyo, Kashiwa, Chiba 277-8581, Japan

^eNihon University, Sakurajosui, Setagaya, Tokyo 156-8550, Japan

^fKochi University, Kochi, Kochi 780-8520, Japan

We have carried out a powder X-ray diffraction investigation on antiferromagnetic Kondo semiconductors $\text{CeRu}_2\text{Al}_{10}$ and $\text{CeOs}_2\text{Al}_{10}$ at low temperatures and under high pressures as well as the structural investigation on single crystal of these compounds. The results of powder X-ray studies of $\text{CeRu}_2\text{Al}_{10}$ and $\text{CeOs}_2\text{Al}_{10}$ indicate that these compounds do not have structural transition at its antiferromagnetic ordering temperature. The results of single crystal structural refinement indicate that the b -axis of this crystal structure is insensitive not only to pressure but also to temperature and that the effect of cooling to Ce–Ce distance for $\text{CeRu}_2\text{Al}_{10}$ is the same as that for $\text{CeOs}_2\text{Al}_{10}$.

DOI: [10.12693/APhysPolA.131.988](https://doi.org/10.12693/APhysPolA.131.988)

PACS/topics: 61.50.Ks

1. Introduction

$\text{CeT}_2\text{Al}_{10}$ ($T = \text{Ru, Os}$) crystallizes in orthorhombic structure (space group $Cmcm$ No. 63) [1]. These compounds have been reported to exhibit antiferromagnetic (AFM) ordering at ordering temperatures (T_N) of $\text{CeRu}_2\text{Al}_{10}$ and $\text{CeOs}_2\text{Al}_{10}$ are 27.3 and 28.7 K, respectively [2, 3]. These compounds are also reported as a Kondo semiconductor, the gap of which is due to the strong c - f hybridization. Optical conductivity studies have confirmed the c - f hybridization gap in $\text{CeRu}_2\text{Al}_{10}$ and in $\text{CeOs}_2\text{Al}_{10}$ are 35 and 45 meV, respectively [4, 5].

These compounds have been extensively studied because of the coexistence of AFM ordering and c - f hybridization gap. Neutron scattering have confirmed the existence of antiferromagnetic ordering in both $\text{CeRu}_2\text{Al}_{10}$ and $\text{CeOs}_2\text{Al}_{10}$ [6–8]. These T_N values are about 100 times higher than that would be expected from the de Gennes law [3]. The electronic instability, which accompanies structural instability, is one possible drive force for the high T_N of $\text{CeRu}_2\text{Al}_{10}$ and $\text{CeOs}_2\text{Al}_{10}$.

The T_N of $\text{CeRu}_2\text{Al}_{10}$ and $\text{CeOs}_2\text{Al}_{10}$ suddenly disappear at a critical pressure (P_C) \approx 4 GPa and 2.5 GPa, respectively [3, 9]. This sudden disappearance, like a first-order transition, implies the possibility of a pressure-induced structural transition near P_C . This study focuses on T_N and on P_C at room temperatures and the effect of cooling to the structure.

In this paper, we report the synchrotron X-ray studies of $\text{CeRu}_2\text{Al}_{10}$ and $\text{CeOs}_2\text{Al}_{10}$ around T_N and as well as those under pressure. We also report the analysis of single crystal structure at 110 K and 300 K.

2. Experimental details

$\text{CeRu}_2\text{Al}_{10}$ and $\text{CeOs}_2\text{Al}_{10}$ were grown by Al self flux method. For the analysis of single crystal structure, we use a piece of single crystal of $\text{CeRu}_2\text{Al}_{10}$ with $50 \mu\text{m} \times 40 \mu\text{m} \times 20 \mu\text{m}$ and that of $\text{CeOs}_2\text{Al}_{10}$ with $70 \mu\text{m} \times 50 \mu\text{m} \times 20 \mu\text{m}$. The measurements of single crystal structure were performed on a Rigaku Saturn724 diffractometer using multi-layer mirror monochromated Mo K_α radiation.

For the experiment of synchrotron powder X-ray diffraction, the single crystals were grinded into a fine powder. The uniform grain was obtained by using sedimentation method. The pressure was applied by diamond anvil pressure cell (DAC). The measurement down to 10 K was cooled with GM refrigerator. The sample was exposed by the beam with a size of $\Phi 100 \mu\text{m}$ in diameter and with a wave length $\lambda \approx 0.62 \text{ \AA}$. Imaging plate was used as a detector. In order to eliminate remaining spots of the Debye ring, a stage of the DAC was oscillated during synchrotron X-ray exposure. The mixture of methanol and ethanol with 4:1 ratio was used as pressure transmission. The pressure was evaluated by ruby fluorescence method.

3. Results and discussions

3.1. Powder X-ray diffraction

Figure 1 shows the X-ray diffraction pattern of $\text{CeRu}_2\text{Al}_{10}$ and $\text{CeOs}_2\text{Al}_{10}$ around P_C at room temperature. The diffraction pattern of $\text{CeRu}_2\text{Al}_{10}$ at 4.2 GPa is

*corresponding author; e-mail:
y_kawamura@mmm.muroran-it.ac.jp

not changed from that at 3.1 GPa except a slight change of peaks position due to the contraction of lattice parameters. Because the P_C of $CeRu_2Al_{10}$ is from 3 GPa to 4 GPa, this result indicates the lack of structural change around P_C at room temperature. In addition, the intensity ratio of the peaks does not change from 3.1 GPa to 4.2 GPa, which implies the lack of structural deformation around P_C at room temperature.

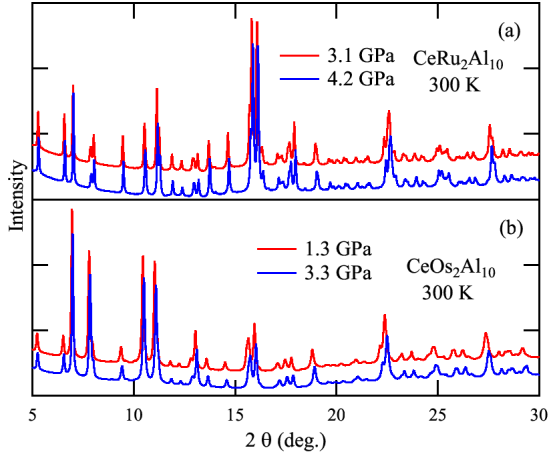


Fig. 1. X-ray diffraction pattern of (a) $CeRu_2Al_{10}$ and (b) $CeOs_2Al_{10}$ at the pressure below P_C (top) and above P_C (bottom).

Similar results can be seen in the X-ray diffraction patterns of $CeOs_2Al_{10}$. The diffraction pattern of $CeOs_2Al_{10}$ at 3.3 GPa is not changed from that at 1.3 GPa except a slight change of peaks position. In addition, the intensity ratio of the peaks does not change from 1.3 GPa to 3.3 GPa. Because the $P_C \approx 2.5$ GPa for $CeOs_2Al_{10}$, these results imply the lack of structural change and deformation around P_C at room temperature.

Although the angles of the peaks of $CeRu_2Al_{10}$ are not so different from that of $CeOs_2Al_{10}$ due to the similar lattice constant, the relative peak intensity of each peaks is considerable different as can be seen in Fig. 1. This difference is due to the difference of the atomic position.

Figure 2 shows the X-ray diffraction pattern around T_N below P_C . Neither peak disappearance nor peak splitting are observed. Furthermore, the intensity of the peak does not change a lot at different temperatures. We note that the background of $CeRu_2Al_{10}$ and $CeOs_2Al_{10}$ is different, which is due to the change of Mylar sheet at the window of GM refrigerator.

We evaluated bulk modulus by the Birch equation of state [10]:

$$P = 3/2B_0 \left[(i/i_0)^{-7} - (i/i_0)^{-5} \right] \times \left\{ 1 + 3/4(B'_0 - 4) \left[(i/i_0)^{-2} - 1 \right] \right\},$$

where B_0 is the bulk modulus, B'_0 is its first pressure derivative, P is the pressure, i ($i = a, b, c$) denotes the lattice parameters, i_0 ($i_0 = a_0, b_0, c_0$) denotes the lattice parameters at ambient pressure. B_0 of a, b, c for

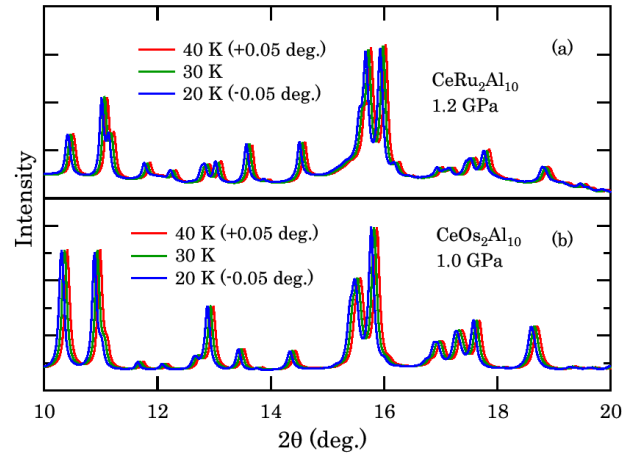


Fig. 2. X-ray diffraction pattern of (a) $CeRu_2Al_{10}$ and (b) $CeOs_2Al_{10}$ at 20 K (left), 30 K (middle), and 40 K (right). The peaks are shifted for clarity as indicated in the parenthesis.

$CeRu_2Al_{10}$ is derived to 101, 128, 97 GPa, respectively. In addition, B_0 of a, b , and c for $CeOs_2Al_{10}$ is derived to 106, 144, and 108 GPa, respectively.

The B_0 of V assuming cubic approximation are among these values; 105 GPa for $CeRu_2Al_{10}$ and 120 GPa for $CeOs_2Al_{10}$ [11]. The large value of b indicates that lattice parameter is insensitive to pressure. The difference of B_0 for b parameter for $CeOs_2Al_{10}$ from the other axis is more distinctive than that of $CeRu_2Al_{10}$.

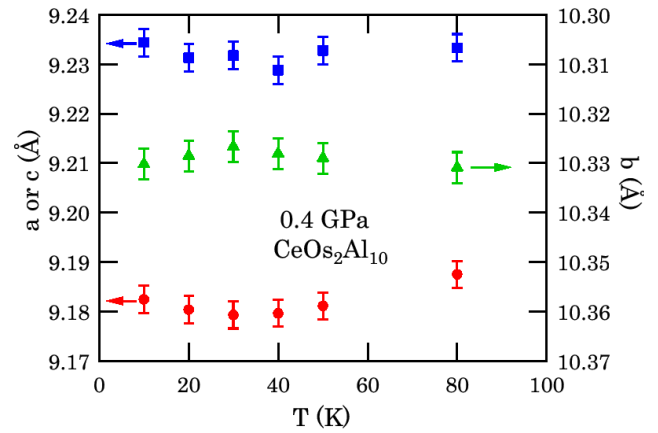


Fig. 3. Lattice parameter a (circle, left axis), b (triangle, right axis), and c (square, left axis) at low temperatures of $CeOs_2Al_{10}$ below P_C .

Figure 3 shows the lattice parameters of $CeOs_2Al_{10}$ at low temperatures below P_C . There is no distinct difference around T_N out of this experimental error attributed to the change of pressure and to the shrink of GM refrigerator by cooling. These results do not contradict to the previous lattice parameters obtained from neutron diffraction with a small anomaly in the case of b parameter at 30 K, because the error bar of neutron diffraction is smaller [12].

3.2. Single crystal analysis

In order to evaluate the effect of cooling on lattice parameters for CeOs₂Al₁₀ and for CeRu₂Al₁₀, we performed single crystal X-ray structure refinement. The refinement parameters of CeRu₂Al₁₀ with $R = 0.028$, $wR = 0.062$, and $S = 1.19$ are compatible to the previous report with $R = 0.043$, $wR = 0.123$, and $S = 1.10$ [13].

Table I shows the lattice parameter of CeRu₂Al₁₀ and CeOs₂Al₁₀ at 300 K and at 110 K. The a and c parameters of CeOs₂Al₁₀ are longer than those of CeRu₂Al₁₀, while the b parameter of CeOs₂Al₁₀ is almost the same as that of CeRu₂Al₁₀. This small b parameter for CeOs₂Al₁₀ induces the large difference of B_0 of b from that of a and c . The differences of lattice parameters a , b , and c at 110 K from those at 300 K for CeRu₂Al₁₀ are 0.23%, 0.12%, 0.21%, respectively. Those for CeOs₂Al₁₀ are 0.18%, 0.09%, 0.21%, respectively.

TABLE I

Lattice parameters and Ce–Ce distance of CeRu₂Al₁₀ and that of CeOs₂Al₁₀. Estimated standard deviations are given in parentheses.

| | CeRu ₂ Al ₁₀ | | CeOs ₂ Al ₁₀ | |
|-----------|------------------------------------|-----------|------------------------------------|-----------|
| | 300 K | 110 K | 300 K | 110 K |
| a [Å] | 9.120(2) | 9.099(3) | 9.139(2) | 9.123(3) |
| b [Å] | 10.268(2) | 10.256(4) | 10.267(3) | 10.258(3) |
| c [Å] | 9.181(2) | 9.162(3) | 9.187(2) | 9.168(3) |
| Ce–Ce [Å] | 5.247 | 5.237 | 5.271 | 5.261 |

Overall, the lattice parameters of CeRu₂Al₁₀ are more sensitive to cooling than those of CeOs₂Al₁₀. This is the same tendency as the B_0 s of CeRu₂Al₁₀ are smaller than those of CeOs₂Al₁₀, where B_0 means the hardness against pressure. The lattice parameters of b for CeRu₂Al₁₀ and CeOs₂Al₁₀ are insensitive to cooling. This tendency is consistent with the results that the lattice parameter of b is insensitive to pressure compared to that of a or c .

Next, we discuss the relation between lattice parameters and physical properties. When CeRu₂Al₁₀ is compared to CeFe₂Al₁₀, the lattice parameter has an anisotropic contraction. We proposed that the shrinkage of lattice parameters a and c is related to the enhancement of the anisotropic c – f hybridization [11]. When CeRu₂Al₁₀ is compared to CeOs₂Al₁₀, the effect of c – f hybridization cannot be related to chemical pressure. Although the c – f hybridization of CeRu₂Al₁₀ is smaller than that of CeOs₂Al₁₀, the volume and the Ce–Ce distance of CeRu₂Al₁₀ are smaller than those of CeOs₂Al₁₀.

On the other hand, the Ce–Ce distance decreases by 0.19% from 300 K to 110 K for both compounds, which indicates the effect of cooling is the same in these compounds. This study reveals that the comparison of temperature dependence of physical properties on CeRu₂Al₁₀ and that on CeOs₂Al₁₀ is fruitful because Ce–Ce distance is essential factor for discussing c – f hybridization and magnetic ordering at T_N .

4. Conclusions

We have investigated structure of CeRu₂Al₁₀ and CeOs₂Al₁₀ at low temperature and at high pressures. Powder X-ray diffraction does not show any hint of structural change or modification at T_N or P_C at room temperature. The structural analysis of the single crystal indicates that the b -axis of this crystal structure is insensitive not only to pressure but also to cooling and that the effect of cooling of Ce–Ce distance for CeRu₂Al₁₀ is the same as that for CeOs₂Al₁₀.

Acknowledgments

The synchrotron radiation experiments were carried out at BL-18C in KEK with the approval of the Photon Factory Program Advisory Committee (proposal Nos. 2013G501, 2015G512). This work was partially supported by JSPS KAKENHI (grant Nos. 15K17687 and 23340092).

References

- [1] V.M.T. Thiede, T. Ebel, W. Jeitschoko, *J. Mater. Chem.* **8**, 125 (1998).
- [2] A.M. Strydom, *Physica B* **404**, 2981 (2009).
- [3] T. Nishioka, Y. Kawamura, T. Takesaka, R. Kobayashi, H. Kato, M. Matsumura, K. Kodama, K. Matsubayashi, Y. Uwatoko, *J. Phys. Soc. Jpn.* **78**, 123705 (2009).
- [4] S. Kimura, T. Iizuka, H. Miyazaki, T. Hajiri, M. Matsunami, T. Mori, A. Irizawa, Y. Muro, J. Kajino, T. Takabatake, *Phys. Rev. B* **84**, 165125 (2011).
- [5] S. Kimura, T. Iizuka, H. Miyazaki, A. Irizawa, Y. Muro, T. Takabatake, *Phys. Rev. Lett.* **106**, 056404 (2011).
- [6] J. Robert, J.M. Mignot, G. Andre, T. Nishioka, R. Kobayashi, M. Matsumura, H. Tanida, D. Tanaka, M. Sera, *Phys. Rev. B* **82**, 100404 (2010).
- [7] D.D. Khalyavin, A.D. Hillier, D.T. Adroja, A.M. Strydom, P. Manuel, L.C. Chapon, P. Peratheepan, K. Knight, P. Deen, C. Ritter, Y. Muro, T. Takabatake, *Phys. Rev. B* **82**, 100405 (2010).
- [8] D.T. Adroja, A.D. Hillier, P.P. Deen, A.M. Strydom, Y. Muro, J. Kajino, W.A. Kockelmann, T. Takabatake, V.K. Anand, J.R. Stewart, J. Taylor, *Phys. Rev. B* **82**, 104405 (2010).
- [9] K. Umeo, T. Ohsuka, Y. Muro, J. Kajino, T. Takabatake, *J. Phys. Soc. Jpn.* **80**, 064709 (2011).
- [10] F. Birch, *Phys. Rev.* **71**, 809 (1947).
- [11] Y. Kawamura, J. Hayashi, K. Takeda, C. Sekine, H. Tanida, M. Sera, T. Nishioka, *J. Phys. Soc. Jpn.* **85**, 044601 (2016).
- [12] D.T. Adroja, A.D. Hillier, Y. Muro, T. Takabatake, A.M. Strydom, A. Bhattacharyya, A.D. Aladin, J.W. Taylor, *Phys. Scr.* **88**, 068505 (2013).
- [13] A.I. Tursina, S.N. Nesterenko, E.V. Murashova, I.V. Chernyshev, H. Noël, Y.D. Seropegin, *Acta Crystallogr. E* **61**, i12 (2005).